The Journal of Engine Research, Vol. 57 (Winter 2020), pp. 27-40

The Journal of Engine Research

Journal Homepage: www.engineresearch.ir

Imaging and Analysis of Auto-Ignition and Heavy Knock in a Full Bore Optical SI Engine

H. Vafamehr[1,2*], A. Mahmoudzadeh Andwari[2], V. Esfahanian[3], G. Hamzehnava[4]

[1] *Faculty of Engineering, University of Nottingham, Nottingham, NG7 2RD, UK, h.vafamehr@ut.ac.ir*
[2] *Vehicle, Fuel and Environment Research Institute, School of Mechanical Engineering, College of Engineering, University of Tehran, Tehran, Iran, amin.mahmoudzadeh@ut.ac.ir*
[3] *Vehicle, Fuel and Environment Research Institute, School of Mechanical Engineering, College of Engineering, University of Tehran, , Tehran, Iran, evahid@ut.ac.ir*
[4] *faculty of Mechanical Engineering, College of Engineering, University of Tehran, Tehran, Iran, hamzehnava@ut.ac.ir*
[*] *Corresponding Author*

ARTICLE INFO

Article history:
Received: 4 January 2020
Accepted: 18 February 2020

Keywords:
Auto-ignition
Knock
Imaging
Optical

ABSTRACT

The work involved a fundamental study of auto-ignition under unusually high knock intensities for an optical spark ignition engine. The single-cylinder research engine adopted included full bore overhead optical access capable of withstanding continuous peak in-cylinder pressures of up to 150bar. A heavy knock was deliberately induced under relatively low loads using inlet air heating and a primary reference fuel blend of reduced octane rating. High-speed chemiluminescence natural light imaging was used together with simultaneous heat release analysis to evaluate the combustion events. Multiple centered auto-ignition events were regularly observed to lead into violent knocking events, with knock intensities above 140 bar observed. The ability to directly image the events associated with such a high magnitude of knock is believed to be a world-first in an optical engine. The multiple centered events were in good agreement with the developing detonation theory proposed elsewhere to be the key mechanism leading to heavy knock in modern downsized SI engines. The accompanying thermodynamic analysis indicated a lack of relation between knock intensity and the remaining unburned mass fraction burned at the onset of the auto-ignition. Spatial analysis of the full series of images captured demonstrated the random location of the initial auto-ignition sites, with new flame kernels forming at these sites and initially growing steadily and suppressing further growth of the main flame front before violent detonation at speeds well over the imaging frequency of the camera.

1) Introduction

Over the past two decades, European automotive CO_2 emissions targets have mainly been met through increased diesel sales. However, the distillation of crude oil results in high proportions of both gasoline and diesel fuel and ultimately this has resulted in Europe becoming "diesel lean" at times. Also, the diesel engine has recently become subject to intense scrutiny in terms of adverse health implications of real-world tailpipe emissions, particularly in urban areas.

To meet future global emissions goals, in the short-to-medium term it will be necessary to improve the fuel consumption of the gasoline engine and in the longer-term source sustainable alternatives to crude oil. Substitutes such as electric and hydrogen fuel cell vehicles are among the alternatives being investigated.

Significant advancements in battery technologies have been made, with full electric now considered the lower-cost route compared to the fuel cell [1], [2]. However, overall, current electric powertrains remain insufficiently advanced to be considered as the dominant source of vehicle propulsion. The most recent annual energy outlook publication compiled by BP suggests electric and plug-in hybrid powertrains will account for less than 10% of the global automotive market in 2035 [3].

The internal combustion engine will, therefore, remain widely used for several decades to come, albeit operating in evolved forms with advanced fuels and some cases as part of a hybrid powertrain, as also acknowledged by the UK automotive council [4].

Engine "downsizing" has been widely adopted over the last decade as one promising method for improving SI engine fuel consumption. The basic principle is to reduce the capacity of the engine and hence enforce a large proportion of operation to higher loads, where under wider open throttle conditions the pumping losses are reduced for a given road load requirement.

Cylinder-specific friction may increase due to higher in-cylinder gas pressures but net friction savings can still be made when the number of cylinders is reduced. To maintain adequate vehicle acceleration and top speed the smaller engine must be pressure-charged and still produce an acceptable transient response.

Overall, for a large family-sized saloon car, it has already been demonstrated that halving total engine capacity from a V6 2.4 liter to a three-cylinder 1.2-liter unit can reduce fuel consumption by up to ~25% with vehicle performance maintained via compound charging [5]. Such downsizing yields significant part-load fuel consumption benefits, but significant challenges remain, including increased high load engine operation under knock limited conditions [6].

The term "right-sizing" has emerged in the last few years [7], [8], which is reflective of the new real-world drive cycles enforcing a much higher proportion of engine operation to higher loads where auto-ignition and knocking combustion remains a key barrier to maximizing thermal efficiency.

The problem of auto-ignition is almost as old as the internal combustion engine itself [7] and still ultimately caps peak thermal efficiency in modern SI engines [8-10], being commonly avoided by selecting a lower compression ratio, retarding the spark timing and/or introducing excess fuel.

Such auto-ignition has been established to be the result of exothermic centers, or "hot spots", leading to auto-ignition of the unburned charge ahead of the developing flame [11-13]; so-called end-gas auto-ignition. However, recent aggressively downsized research engines of very high specific output have additionally experienced pre-ignition combustion at low engine speeds and high loads (>15 bar BMEP).

Previously pre-ignition was most commonly associated with higher engine speeds when the components within the combustion chamber are typically at their hottest. Hence such pre-ignition was at first unexpected, arising below the auto-ignition temperature of the charge and occurring in a highly sporadic manner in short violent bursts in an "on-off" pattern, with sometimes tens of thousands of cycles in-between events [14].

This phenomenon widely referred to as Low-Speed Pre-Ignition (LSPI) and "Super-Knock", has been associated with low-to-moderate thermal gradients within the unburned charge leading to developing detonation events. Ultimately, this may produce multiple high frequency and intensity pressure waves within the cylinder that may interact and ultimately destroy the engine.

The time to trigger the auto-ignition chemistry of a given mixture under known physical conditions provides a useful relative measure of the expected onset and intensity of such events. This auto-ignition delay period cannot be accurately measured directly in real engines due to the complex nature of the combustion process [10].

The delay period is therefore typically estimated using simplified chemical kinetic schemes [15-18] and/or empirical measurements obtained in idealized rapid compression machines or combustion chambers [11] [19-22].

Researchers at the University of Leeds and Shell [23] have recently postulated that such Super-Knock events originate from a resonance between acoustic waves emitted by an auto-igniting hot spot and a reaction wave that propagates along negative temperature gradients in the fuel-air charge. The theory is based upon the assumption that the temperature gradient extends smoothly over sufficient length across the turbulent flow field. Subsequently, localized detonations may develop which are then able to violently ignite the remaining unburned charge in timescales of less than a millisecond. Ultimately, this can lead to catastrophic mechanical engine failure. Peters and co-workers[13], [14] extended this theory developed at Leeds/Shell to at least partially attribute the random nature of the events to the stochastic nature of the in-cylinder turbulence.

In the other study by Pan [15] the results show that as the decreases of octane number, knocking onset is significantly advanced due to the enhancement of low-temperature chemical reactivity.

Consequently, more auto-ignition centers appear at the hot exhaust valve side and even cool intake valve side at a very low octane number. But for the knocking intensity, it does not always show a proportional correlation with octane number during super-knock. However, some uncertainty remains around the triggering of these events. The pre-ignition typically occurs well below the auto-ignition temperature of the bulk charge, considered to be indicative of a deflagration caused by an exothermic center with the high-temperature gradient across it [16]. It has also been suggested that the auto-ignition might be caused by a localized volume of charge with particularly low auto-ignition temperature, such as an evaporating droplet of lubricant (or mixtures of fuel and oil due to wall impingement of a directly injected fuel spray). Such droplets, of relatively low octane number (and high cetane number), have been suggested to cause the formation of the deflagration site(s) leading to pre-ignition and Super-Knock.

To this end, Dahnz et al. [17] produced a simple pre-ignition model to qualify the effects of a low-octane droplet within the main (high-octane) charge. It was found that a region existed where, given sufficient droplet temperature, ignition could be initiated below the bulk auto-ignition temperature of the main charge. When developing their theory Kalghatghi and Bradley [12] used pressure data from real engine Super-Knock cycles to show that gas-phase pre-ignition of an evaporating lubricant droplet could be possible, assuming that the lubricant droplet was substantially more reactive than n-heptane. In recent work by South-west Research Institute many lubricants were found to meet this condition [18].

With the complex nature of cyclic variations in SI engines influenced by varying turbulence, charge homogeneity, wall temperatures, deposit conditions, fuel and oil properties [14], [17]–[20] it is quite probable that the stochastic pre-ignition event is caused by a combination of phenomena. However, the theory of an increased likelihood of auto-ignition occurring due to suspended oil droplets has widely gained credibility. Amann et al. [21] found that, during a sequence of Super-Knock events in a multi-cylinder engine, the air-fuel ratio was significantly reduced compared to the calibrated air-fuel ratio. When extremely high intensity knocking combustion was artificially induced by intermittently advancing the spark timing, the same trend in the air-fuel ratio was not observed. This observation was therefore attributed to the accumulation of lubricant during normal engine running and its subsequent release from the piston top-land crevice during Super-Knock events. In other recent work by some of the current authors [22], oil was deliberately directly injected into the charge of a full bore optical engine, with the transport properties of the lubricant indicated to have some effect on the likelihood of pre-ignition and knock occurring. These observations were in good agreement with those reported simultaneously elsewhere in a full metal engine by Wellings and co-workers using identical lubricant blends [23].

In existing spark-ignition engines the onset of knock is sometimes avoided by running fuel-rich [24], [25], where the charge cooling properties and a reduced ratio of specific heats suppresses the onset of knocking combustion. This is undertaken at the expense of poor fuel consumption and vastly increased tailpipe emissions (given the three-way catalyst is no longer effective). Nonetheless, the slightly rich combustion may help maximize full load output.

Also, excess fuel is commonly utilized at higher speeds and loads to limit exhaust gas temperatures and protect the exhaust components. Such operation is not sustainable, particularly in light of the real-world driving cycles currently being proposed within the EU and elsewhere to cover a wider area of engine operation. Furthermore, questions remain over the consequences of rich operation during Super-Knock in downsized spark ignition engines, where pre-ignition may lead to a sudden violent knocking event and the presence of excess fuel (and/or inappropriate fuel stratification) could be detrimental. The complexity is arguably further exacerbated by emerging future fuels, where a fuel such as ethanol with high sensitivity (i.e. relatively high RON but low MON) may help reduce the onset of knock[26]–[28] but could theoretically exacerbate sporadic pre-ignition under certain conditions due to the increased pre-ignition tendency as indicated by the lower MON rating [29].

The currently reported work was concerned with providing further insights into the events associated with a severe knock. The well-cited developing detonation theory suggests that the most violent events in SI engines must be associated with a chain of auto-ignition events, with multiple centers occurring in such short timescales that cannot be captured using existing optical equipment. However, the ability to monitor trends over several cycles should be allowed some qualitative extraction of any repetition within the events.

2) Materials and methods

2-1) Experimental engine

A custom-made research engine with a unique optical arrangement was used for this research. The engine was based on the bottom end from a Lister-Petter TS1 and combined full-bore overhead access with a semi-traditional poppet-valve valvetrain. The engine has been designed with a special window mounting, including a large fused silica window mounted in a softer aluminum sleeve (with a thin layer of special high-temperature sealant between the silica and metal). This special mounting has been developed in-house to withstand continuous peak in-cylinder pressures of up to 150bar, with short-term transient deviations of up to 200bar previously tolerated. The side-mounted poppet intake valves allowed for intake boosting and provided a forward tumble flow pattern that was representative of a real production engine. The original design composed of two exhaust valves, but in the current study, only one exhaust valve was used. A cross-sectional view of the cylinder head is presented in Figure 1.

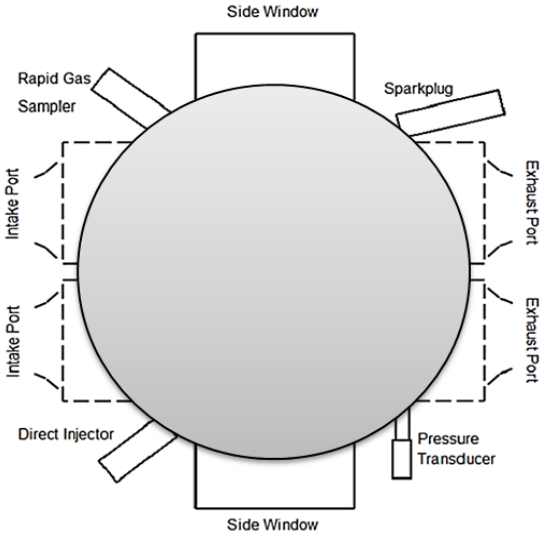

Figure 1: Overhead schematic of the cylinder head concept

Similar research engines exist, most notably at Sandia National Laboratories. However, the engine at Sandia featured intake and exhaust valves that were flush with the cylinder wall. This accommodated optical access to the entire combustion chamber but limited the compression ratio to approximately 5.3:1[30]. The engine used in this research featured a compression ratio of 8.4:1. This was achieved by recessing the intake and exhaust valves into the side-wall of the cylinder. This created hidden regions within the combustion chamber that have been referred to as “valve-pockets”. While the lack of optical access to these regions is not ideal, it was accepted because the pockets remained inaccessible during much of the combustion period e[22].

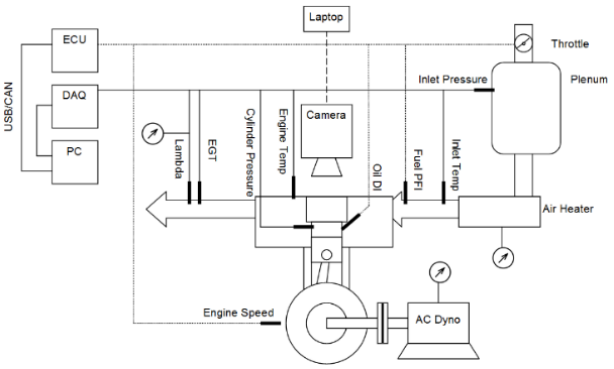

Figure 2: Schematic of the experimental setup

In addition to the high level of optical access, the engine was designed to withstand continuous peak in-cylinder pressures of up to 150bar. On a transient basis, knocking combustion with a peak in-cylinder pressure of 204 bar has been recorded without damage, with the associated in-cylinder pressure data for this cycle shown in Figure 3.

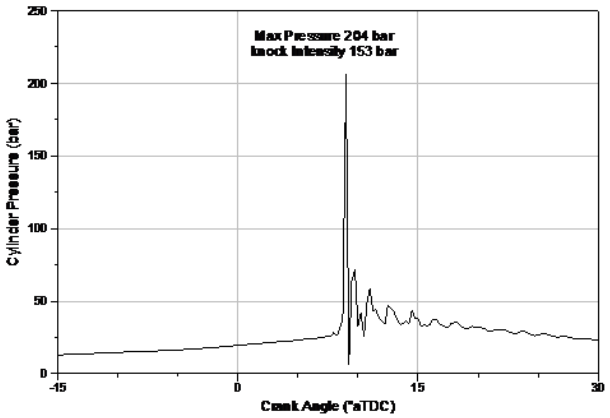

Figure 3: In-cylinder pressure against crank angle showing the heaviest recorded knocking cycle

Key geometric features of the engine are presented in Table 1. The unit was coupled to an eddy-current dynamometer with a maximum power absorption/supply of 10 kW. The ignition system comprised of an NGK ER9EH 8mm spark plug supplied by a Bosch P100T ignition coil. In terms of thermodynamic measurements, an AVL GH14DK pressure transducer was fitted flush within the cylinder head and a piezo-resistive sensor was used to measure the intake plenum pressure. These were both sampled at 4 samples per crank angle degree via a digital shaft encoder coupled to the intake camshaft. The signals were logged using a high-speed USB data-logging card. Engine operating temperatures were measured via a separate low-speed card at 1 Hz. Being air-cooled, the cylinder head and liner temperatures were closely monitored throughout testing. The head temperature was measured at two locations: Firstly at the injector tip and secondly at the exhaust valve bridge.

The measurements sampled by both cards were logged and processed via an in-house Matlab based system. The mass fraction burned and rate of heat release data calculated using the well-known Rassweiler and Withrow method [31]. Pre-ignition cycles were defined as cycles where the rate of heat release had exceeded 1 J/CA before the spark timing. Knock intensity measurements were calculated by applying a mean value filter to the cylinder pressure signal. The maximum value of the filtered signal was then taken to be the maximum knock intensity of that cycle.

Table 1: Table of key engine geometric parameters

Parameter	Value
Bore (mm)	95
Stroke (mm)	89
Swept Volume (cc)	631
Clearance Height (mm)	9
Geometric Compression Ratio	8.4:1
Exhaust Duration (deg. CA)	230
Exhaust MOP (°bTDC)	105
Exhaust Valve Lift (mm)	5
Standard Valve Overlap (deg. CA)	25
Intake Duration (deg. CA)	230
Inlet MOP (°aTDC)	100
Inlet Valve Lift (mm)	5
Con-Rod Length (mm)	165.16

2-2) Engine warm-up and test procedure

The engine was air-cooled, which was considered acceptable given the limited time running experienced in optical engines to avoid window fouling. The engine was cooled down until the cylinder head temperature reached 85°C(±2°C) as measured at the DI tip and 90°C as measured at the exhaust valve bridge.

Each test session started with the engine at this temperature. The desired engine test conditions were then set and the engine test procedure started. The test procedure involved a 75second warm-up followed immediately by a data capture period of 100 cycles. Thermodynamic results were averaged over 3 sets of 100 cycles for each test condition.

The sump oil temperature remained relatively low throughout testing and was typically between 20 and 40°C. The sump lubricant temperature was not found to influence the frequency of the induced pre-ignition[22].

Before any further data acquisition, the engine was stopped and allowed to cool until the initial head temperatures of 85°C and 90°C was reached (it was necessary to operate in such a manner due to the lack of water cooling and the need to maintain the same starting thermal conditions when considering auto-ignition).

2-3) Optical Setup

Images of the visible light from combustion were captured via the overhead window as shown in Figure 4. An NAC MEMRECAM fx6000 high-speed

video camera was used at 6000 frames per second (fps), with a resolution of 512 x 384 pixels. All cycles presented in this paper were imaged at 6000fps with an exposure time of 167µs. The internal memory of the camera allowed for a total of 10,000 frames to be recorded before the data had to be downloaded onto a laptop. At 1200rpm this allowed for 16 cycles to be recorded in a single test. Due to the large variation in the intensity of the light emission from combustion between cycles, the gain was adjusted for each cycle to improve the clarity of the images. In the second stage, a weight factor should be specified for each significant parameter defined by ANOVA. To do this, linear regression analysis is carried out to obtain the impact factor of each parameter at different engine operation modes. Input parameters for the models are given according to their importance by applying the weight factors so that the sum of weight factors of the parameters is equal to 1.

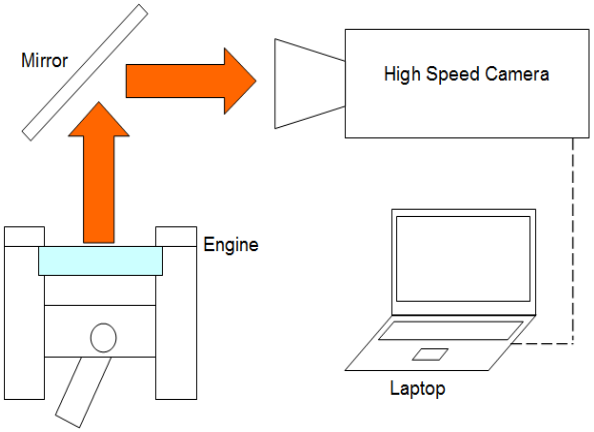

Figure 4: Schematic of the experimental setup for combustion imaging Performance

3) Baseline Heavy Engine Knock

The term "knock" refers to the heavy metallic "pinging" noise that originates from acoustic pressure waves initiated by the auto-ignition events. These shockwaves are caused by uncontrolled combustion of part or all of the unburned charge. The problem of knock is almost as old as the SI engine, with the associated limit to engine output reported for over130 years[32]. Before extensive research on knock in the early 1990s [9], [16], [19], [33], there were two main theories for the cause of end-gas knock; namely homogenous auto-ignition and detonation theory [16], [34]. The homogenous auto-ignition theory was first reported by Ricardo [35] as a direct limit to engine output and efficiency. Elsewhere, the detonation theory [36] described knocking as a result of the exponential acceleration of the normal flame resulting in detonation. However, such simplified theories were unable to account for all of the observed behavior of knocking combustion [32], [37]. In the 1990s a theory of heterogeneous auto-ignition, initiated at discrete points within the end-gas (so-called "hot-spots"), was proposed by Konig and Sheppard et al.[9], [19], [33], [37] . These workers applied the three modes of exothermic reaction propagation originally described by Zel'dovich for one-dimensional shock tubes to exothermic centers within a two-dimensional combustion chamber end-gas region. The three modes of reaction propagation described by Zel'dovich are outlined in Table 2, with the likelihood of occurrence of each mode directly linked to the thermal gradient across the hot spot.

Table 2: Overview of Zel'dovich's modes of exothermic reaction propagation and modeled knock intensities by Konig and Sheppard et al.

Flame Propagation Regime	Temperature Gradient across Exothermic Centre	Modeled Knock Intensity
Deflagration	~125K/mm (High)	Low to Moderate
Thermal Explosion	~1.25K/mm (Low)	Moderate
Developing Detonation	~12.5K/mm (Intermediate)	Heavy

Figure 5 shows the relation between the knock intensity of a knocking combustion cycle and the crank angle location of maximum heat realise (knock onset for knocking cycles) for 100 consecutive cycles. From the data in this graph it can be seen that on the right-hand-side of the graph, where the knock intensity is lower and heat release started after ignition, there is a link between the timing of knock onset and the resulting knock intensity. In this area, the main reason for knock is normal flam propagation after ignition followed by end gas deflagration.
It could be depicted from the graph when pre-ignition and leading knock occur closer to the TDC, corresponding KI value is higher due to the higher temperature and in-cylinder pressure. For instance, Cycles 54 and 74 were selected as shown in the graph. In cycle 54, as the location of the maximum average in-cylinder pressure

gradient(~14°aTDC) is closer to TDC, related KI value is significantly higher than cycle 74 which has KI value of 0.7 at 26°aTDC. The lower graph shows the rate of heat release for the same cycles. These ROHR signals were used to detect pre-ignition by setting a threshold that was above the noise level of 5J/CA. Once the ROHR of a cycle had reached this threshold it was considered to have ignited. If a cycle reached this threshold before the spark timing (-17°aTDC) then it assumed to be a pre-ignition cycle. Therefore there is clear evidence that all pre-ignition cycles have a KI value of more than 4 bar.

The same result reported in the study by Konig and Sheppard. They experimentally have shown, for a given engine running condition, the knock intensity of a knocking combustion cycle was closely linked to the crank angle location of knock onset[33]. The crank angle location of knock onset may be approximated by the location of the maximum average in-cylinder pressure gradient (CA_dP/dCA_max).

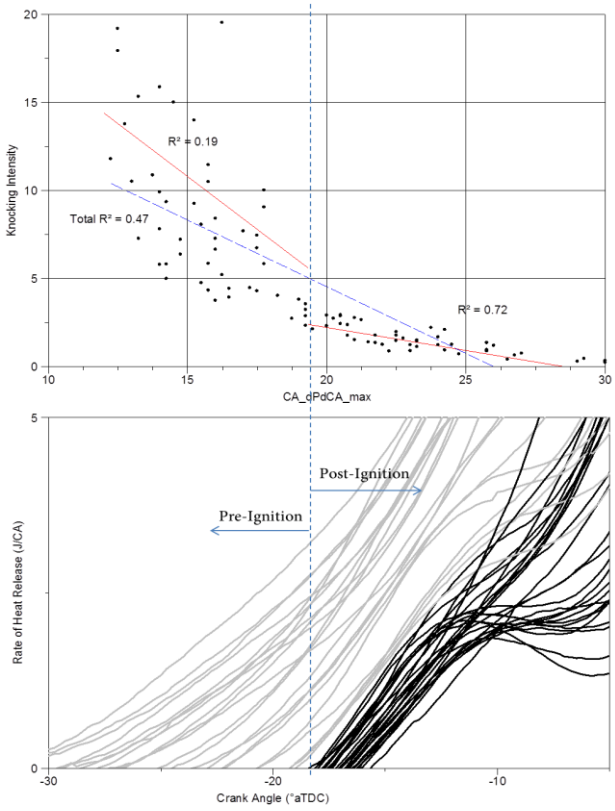

Figure 5: Knock intensity against the location of the maximum rate of change of pressure

As reported in the previous study, knock intensity is strongly influenced by the crank angle at the onset of knock [33]. This theory is completely in agreement with figure 5, where cycles with higher knock intensity are closer to TDC. So it could be concluded that knock intensity is correlated strongly with the temperature and pressure of the unburned gas at the onset of the auto-ignition. This dominated the effects of any other parameters. To this end, Figure 6 shows the knock intensity of different cycles with various conditions plotted versus unburned mass fraction at the onset of auto-ignition. From data presented in figure 6, heavy knocking cycles with KI over 10 bar (29 cycles), were selected. More investigation on these cycles exposed the on-off behavior of knocking cycles. It means 90% of heavy knocking cycles followed by normal or light knocking cycles.

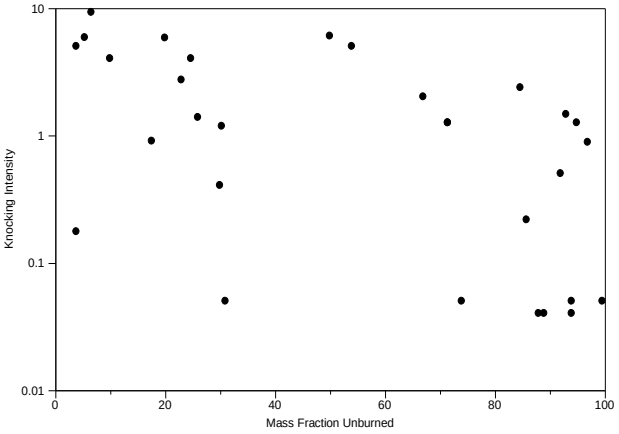

Figure 6: Knock intensity versus unburned mass at the onset of auto-ignition

Figure 7(A) shows the relation between the knock intensity of cycle i and next cycle i+1. As highlighted on the graph, cycle with high KI value followed by cycle with notably lower knock intensity.

Figure 7(B) demonstrates the KI for all selected cycles. Shown in figure 8 is an optical analysis of light and heavy knocking cycles in different crank angles captured by using a fast speed camera at 6000 fps.

As it has been discussed previously, in the cycle with higher knock intensity (37 bar), end gas auto-ignition happened after 8.1 °aTDC. On the other hand, the cycle with lower knock intensity (KI = 3.2) autoignition started considerably later around 17°aTDC. Also, cycles with the same KI can have different onset of pre-ignition as it is not a dominant factor and all these shreds of evidence show the stochastic nature of combustion and cycle-by-cycle variation in the spark-ignition engine [38]. Shown in figure 9, three cycles with KI around 16 bar. In cycle A, detonation happened at crank angle 8.1°aTDC while for cycles B and C it happened at 13.5°aTDC and16.2°aTDC respectively.

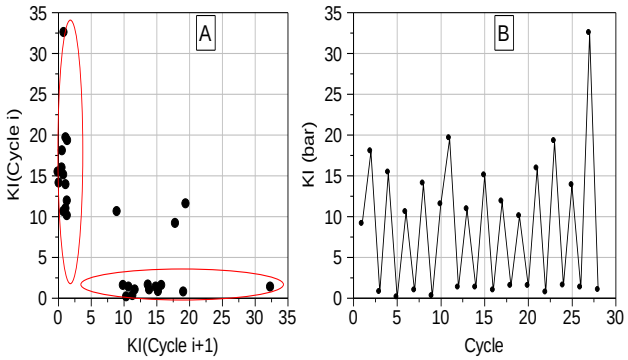

Figure 7: On-Off behaviour of heavy knocking cycles

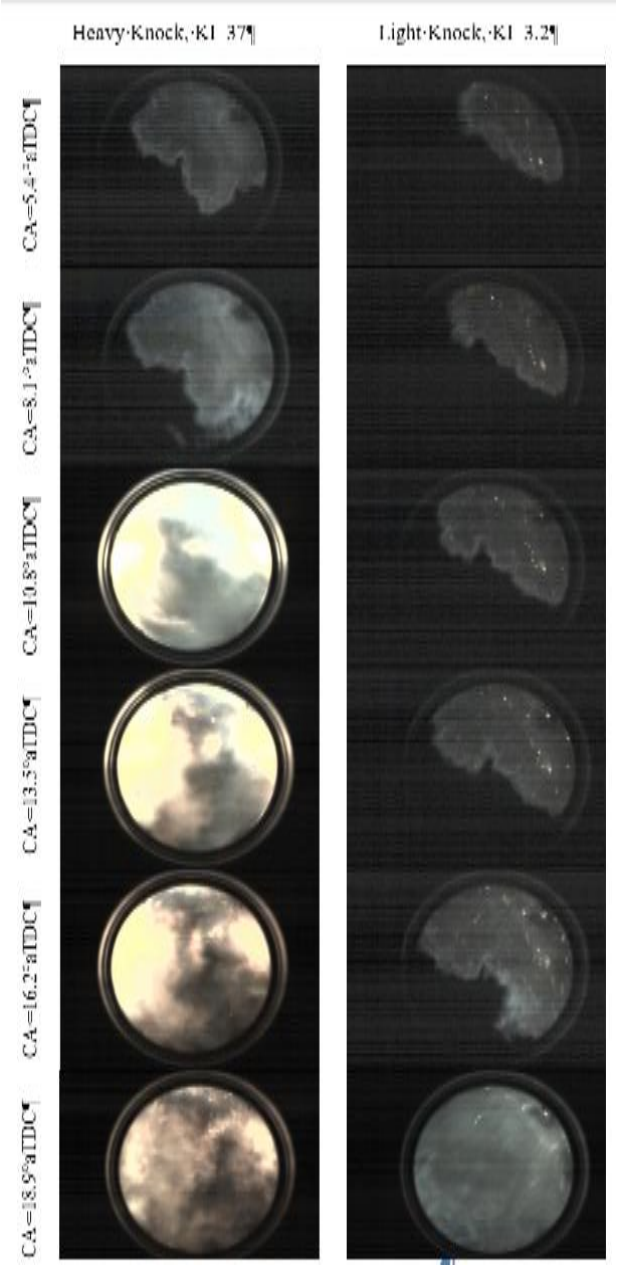

Figure 8: Optical analysis of heavy vs light knock

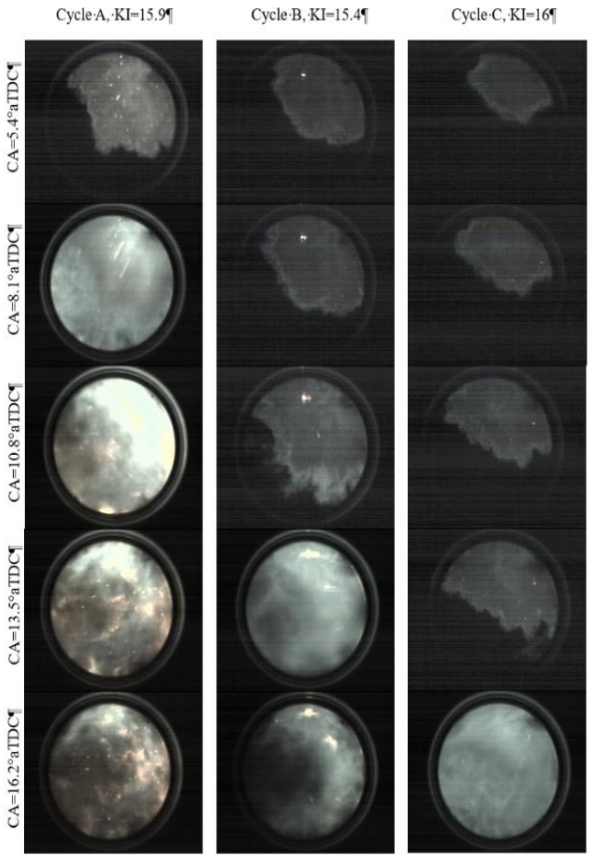

Figure 9: Cycles with same KI but different timing for onset of auto-ignition

4) Pre-ignition caused by Oil droplet in the combustion chamber

During heavy knock tests, there was some optical evidence shows burning oil could cause pre-ignition in the combustion chamber. There are many reasons for engine oil to come to the combustion chamber naturally; the main reason could be the mall function of piston rings. Also overfilling the engine oil could result in a higher level of oil in the engine oil reservoir which could come to the combustion chamber by touching the bottom part of the piston. Figure 10 shows both thermodynamic and optical data for a cycle with a huge amount of oil in the combustion chamber. The photo has been taken exactly at spark timing as it is shown in the top right corner of the picture. Remarkably, pre-ignition has happened far before the spark plug ignites and the flame has been propagated almost one-third of the combustion chamber by that time. High pressure and temperature of this pre-ignition, later led to heavy knock. As the graph shows both normal and heavy knocking cycles, the cycles with oil have higher in-cylinder pressure and knock intensity of 27 bar.

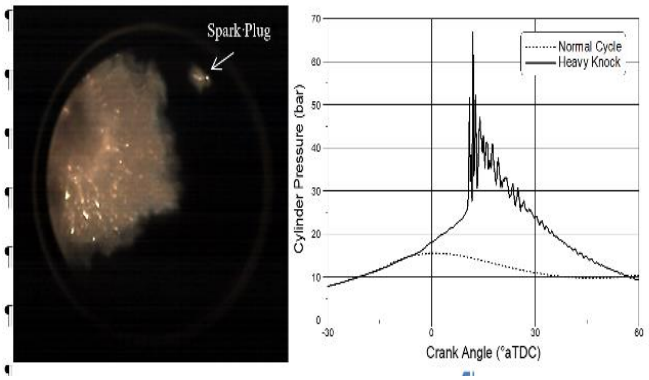

Figure 10: Heavy knock caused by oil in the combustion chamber

In addition to the above discussion about leaking the engine oil in the combustion chamber, after considering more than 500 cycles with optical data another theory came up. A more precise investigation shows a considerable amount of engine oil in the combustion chamber in the cycle after a heavy knock. Figure 11 shows some optical shreds of evidence of oil droplets present in the combustion chamber after a heavy knock. As it is clearly shown, all shining particles inside the flame front are burning oil droplets. Interestingly, all cycles after heavy knock which have a huge amount of oil, have less knock intensity in comparison to the previous cycle. The reason could be the cooling effect of oil droplets in the combustion chamber and lower pressure and temperature of unburned gas. In most samples, knock intensity reduced more than 50% in the next cycle.

It has been proved that heavy knock would make pressure waves traveling at the speed of sound in the combustion chamber [39][40]. These pressure waves make a vibration in piston and piston rings could not work properly to seal the combustion chamber. In consequence, loads of oil droplets would exist in the next cycle. This observation is in agreement with a recent study by Kawahara [41]. After visualization of auto-ignition and pressure waves that occurred during knocking, he noted that the auto-ignition and pressure waves caused the thermal boundary layer to breakdown near the cylinder wall and piston head, therefore combustion of the lubricant oil grease was visible inside the burned gas region.

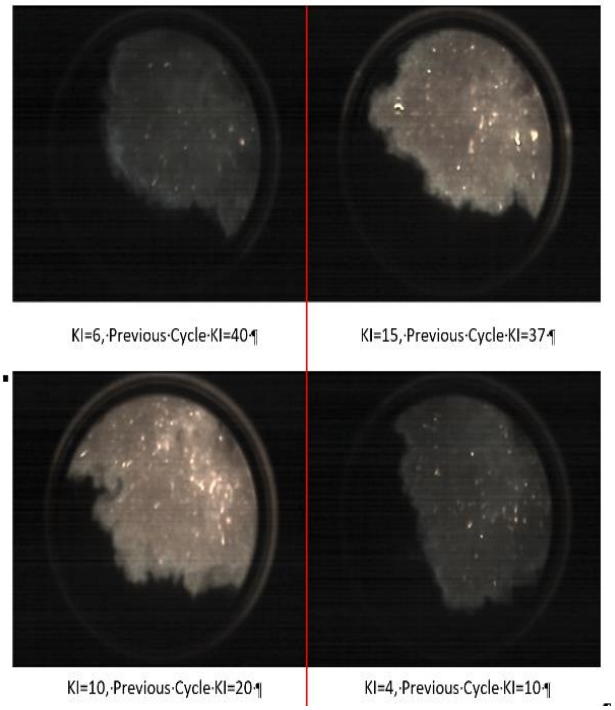

Figure 11: Optical evidence of oil existence in the combustion chamber after a heavy knock

5) Locations of auto-ignition onset inside the combustion chamber

In the experimental investigation, more than 500 cycles were captured using natural light photography. Although the frame rate of the camera was not adequate to determine the knock inducing process, some indication of end-gas auto-ignition before knock could be observed in all knocking cycles. In most of the cycles, multiple auto-ignition sites appeared as shown in figure 12.

Figure 12: Blown-up intensified view of the multiple auto-ignition initiation sites observed during the baseline heavy knock cycle

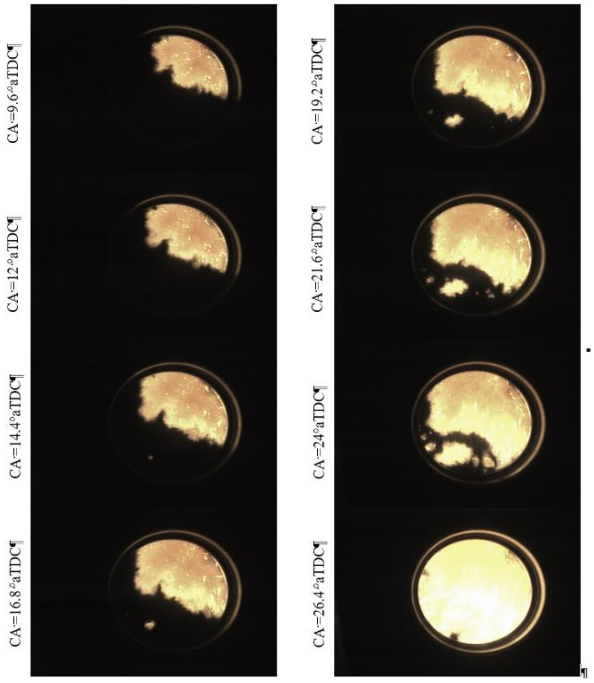

Figure 13: multiple auto-ignition sites

Such multiple centers were regularly noted under heavy knocking conditions, in good agreement with prior developing detonation theory [9], [12], [19]. Also, Kawahara [41] noted that the explosive detonation reaction may be composed of many individual detonation reactions. Furthermore, the end zone becomes sufficiently conditioned or sensitive that many separate areas become centers for starting the detonation reaction.

The locations of auto-ignition were found to vary between cycles. All photos have been examined and classified in terms of three auto-ignition site locations:

a) Auto-ignition onset within the end-gas at a location between the flame front and the cylinder wall.

b) Auto-ignition onset close the cylinder wall (more like end-gas auto-ignition).

c) Auto-ignition onset near the exhaust port.

The examples in figure 14 show the distribution of auto-ignition onset locations for three different cases.

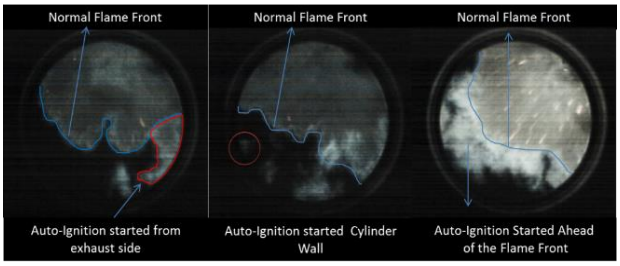

Figure 14: Demonstration of different auto-ignition site locations

Figure 15 illustrate the engine overhead schematic and percentage of auto-ignition in different locations. More than half of the auto-ignitions happened ahead of flame front as pressure and temperature of unburned gas are continuously increasing. Also end-gas knock has been counted in this section. Hot temperature of exhaust port and the tendency of air-fuel mixture to auto-ignite in higher temperatures is the reason for third of the cycles (32%) to have onset of auto-ignition close to exhaust port. The occurrence of auto-ignition near the walls is less likely. In the study by Gerhard Konig[42] he noted this is possibly associated with a lessen concentration of reactant, due to boundary layer hydrocarbons and comparatively lower cylinder wall temperature.

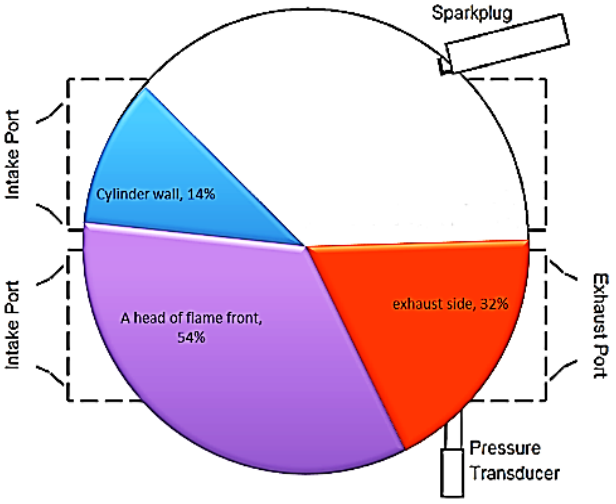

Figure 15: Overhead schematic of the cylinder head, auto-ignition locations.

6) Conclusion

A heavy knock was deliberately induced under relatively low loads using inlet air heating and a primary reference fuel blend of reduced octane rating. High-speed chemiluminescence natural light imaging was used together with simultaneous heat release analysis to evaluate the combustion events.

It was observed that knock intensity is more affected by the crank angle of auto-ignition onset. Cycles with Pre-ignition (and/or auto-ignition) onset closer to TDC have higher knock intensity due to higher pressure and temperature. Analysis of the unburned mass fraction at the beginning of the pre-ignition showed no relation to knock intensity under any of the conditions studied.

Naturally released lubricant droplets were observed in cycles following a high knock and appeared to initiate pre-ignition in subsequent

cycles. The results showed that 90% of heavy knocking cycles were followed by normal or light knocking cycles which presented characteristics of the previously reported "on-off-on" nature of super-knock.

Full bore chemiluminescence imaging confirmed multiple centered auto-ignition sites and the relationships between the location of the auto-ignition sites and knock intensity. The optical analysis showed 54% of auto-ignition events initiated ahead of the flame front due to higher pressure and temperature in this zone, which is favorable for auto-ignition. Also, 32% of auto ignitions happened near the exhaust side due to the higher temperature of this area.

Acknowledgment

The authors would like to thank the personnel of the Centre of Advanced Powertrain and Fuels (CAPF) at Brunel University London for their support in the experimental part of this work.

Fuel Properties

Property	Iso-Octane	n-Heptane
Chemical Formula	C8H18	C7H16
Boiling point at 1 atm (°c)	99.2	98.4
Enthalpy of vaporisation at 298.15 K (MJ/Kmol)	35.14	36.63
Density at 25°C (Kg/m^3)	690.4	681.5
Latent Heat of Vaporisation(kJ/kg)	308	318
Reid Vapour Pressure (bar)	0.52	0.12
Oxygen Content by Weight (%)	0	0
Volumetric Energy Content (MJ/l)	30.6	30.48
RON (MON)	100 (100)	0 (0)

Nomenclature

Symbol	Description
aTDC	after Top Dead Centre
AFR	Air-to-Fuel Ratio
bTDC	before Top Dead Centre
BMEP	Brake Mean Effective Pressure
BSFC	Brake Specific Fuel Consumption
CA	Crank Angle
CCV	Cycle-by-Cycle Variation
CO_2	Carbon (IV) Oxide
COV	Coefficient of Variation
DI	Direct Injection
EU	European Union
ID	Injection Duration
IMEP	Indicated Mean Effective Pressure
MFB	Mass Fraction Burned
NEDC	New European Drive Cycle
PFI	Port Fuel Injection
RON	Research Octane Number
SOI	Start of Injection
SI	Spark Ignition
TDC	Top Dead Centre
VVT	Variable Valve Timing
WOT	Wide Open Throttle
λ	Relative air-to-fuel ratio

References

[1] G. J. Offer, D. Howey, M. Contestabile, R. Clague, and N. P. Brandon, "Comparative analysis of battery electric, hydrogen fuel cell and hybrid vehicles in a future sustainable road transport system," *Energy Policy*, vol. 38, no. 1, pp. 24–29, 2010.

[2] M. Granovskii, I. Dincer, and M. A. Rosen, "Economic and environmental comparison of conventional, hybrid, electric and hydrogen fuel cell vehicles," *J. Power Sources*, vol. 159, no. 2, pp. 1186–1193, 2006.

[3] *BP Energy Outlook 2017 edition*. .

[4]"1. Automotive Council. [Online] http://www.automotivecouncil.co.uk/wp-content/uploads/2013/09/Passenger-car.jpg." .

[5] G. Lumsden, D. OudeNijeweme, N. Fraser, and H. Blaxill, "Development of a Turbocharged Direct Injection Downsizing Demonstrator Engine," *SAE Int. J. Engines*, vol. 2, no. 1, pp. 1420–1432, Apr. 2009.

[6] J. W. G. Turner, A. Popplewell, R. Patel, T. R. Johnson, N. J. Darnton, S. Richardson, S. W. Bredda, R. J. Tudor, C. I. Bithell, R. Jackson, S. M. Remmert, R. F. Cracknell, J. X. Fernandes, A. G. J. Lewis, S. Akehurst, C. J. Brace, C. Copeland, R. Martinez-Botas, A. Romagnoli, and A. A. Burluka, "Ultra Boost for Economy: Extending the Limits of Extreme Engine Downsizing," *SAE Int. J. Engines*, vol. 7, no. 1, pp. 387–417, Apr. 2014.

[7] C. Stan, a. Stanciu, R. Troeger, L. Martorano, C. Tarantino, M. Antonelli, and R. Lensi, "Direct Injection Concept as a Support of Engine Down-Sizing.," *SAE Tech. Pap. 2003-01-0541*, vol. 2003, no. 724, 2003.

[8] J. L. J. Liu and H. P. H. Peng, "Control optimization for a power-split hybrid vehicle," *2006 Am. Control Conf.*, pp. 466–471, 2006.
[9] G. König, R. R. Maly, D. Bradley, a K. C. Lau, and C. G. W. Sheppard, "Role of Exothermic Centres on Knock Initiation and Knock Damage," p. 902136, 1990.
[10] S. Cheng, Y. Yang, M. J. Brear, D. Kang, S. Bohac, and A. L. Boehman, "Autoignition of pentane isomers in a spark-ignition engine," *Proc. Combust. Inst.*, vol. 36, no. 3, pp. 3499–3506, 2015.
[11] L. Bates and D. Bradley, "Deflagrative, auto-ignitive, and detonative propagation regimes in engines," *Combust. Flame*, vol. 175, pp. 118–122, 2017.
[12] G. T. Kalghatgi and D. Bradley, "Pre-ignition and 'super-knock' in turbo-charged spark-ignition engines," *Int. J. Engine Res.*, vol. 13, no. 4, pp. 399–414, 2012.
[13] N. Peters and B. Kerschgens, "Super-Knock Prediction Using a Refined Theory of Turbulence," *SAE Int. J. Engines*, vol. 6, pp. 953–967, 2013.
[14] L. Bates, D. Bradley, G. Paczko, and N. Peters, "Engine Hot Spots: Modes of Auto-ignition and Reaction Propagation," *Combust. Flame*, 2015.
[15] J. Pan, H. Wei, G. Shu, M. Pan, D. Feng, and N. Li, "LES analysis for auto-ignition induced abnormal combustion based on a downsized SI engine," *Appl. Energy*, vol. 191, pp. 183–192, 2017.
[16] J. Pan and C. G. W. Sheppard, "A Theoretical and Experimental Study of the Modes of End Gas Autoignition Leading to Knock in S. I. Engines," 1994.
[17] C. Dahnz, K.-M. Han, U. Spicher, M. Magar, R. Schiessl, and U. Maas, "Investigations on Pre-Ignition in Highly Supercharged SI Engines," *SAE Int. J. Engines*, vol. 3, no. 1, pp. 214–224, 2010.
[18] M. Amann, T. Alger, B. Westmoreland, and A. Rothmaier, "The Effects of Piston Crevices and Injection Strategy on Low-Speed Pre-Ignition in Boosted SI Engines," *SAE Int. J. Engines*, vol. 5, no. 3, pp. 1216–1228, Apr. 2012.
[19] J. Pan, C. G. W. Sheppard, A. Tindall, M. Berzins, S. V. Pennington, and J. M. Ware, "End Gas Inhomogeneity, Autoignition and Knock," 1998.
[20] J. . Griffiths, J. . MacNamara, C. G. . Sheppard, D. . Turton, and B. . Whitaker, "The relationship of knock during controlled autoignition to temperature inhomogeneities and fuel reactivity," *Fuel*, vol. 81, no. 17, pp. 2219–2225, 2002.
[21] M. Amann, D. Mehta, and T. Alger, "Engine Operating Condition and Gasoline Fuel Composition Effects on Low-Speed Pre-Ignition in High-Performance Spark Ignited Gasoline Engines," *SAE Int. J. Engines*, vol. 4, no. 1, pp. 274–285, Apr. 2011.
[22] S. F. Dingle, A. Cairns, H. Zhao, J. Williams, O. Williams, and R. Ali, "Lubricant Induced Pre-Ignition in an Optical SI Engine," 2014.
[23] O. Welling, J. Moss, J. Williams, and N. Collings, "Measuring the Impact of Engine Oils and Fuels on Low-Speed Pre-Ignition in Downsized Engines," *SAE Int. J. Fuels Lubr.*, vol. 7, pp. 1–8, 2014.
[24] A. Cairns, N. Fraser, and H. Blaxill, "Pre Versus Post Compressor Supply of Cooled EGR for Full Load Fuel Economy in Turbocharged Gasoline Engines," in *SAE Technical Paper*, 2008.
[25] H. Nose, T. Inoue, S. Katagiri, A. Sakai, T. Kawasaki, and M. Okamura, "Fuel Enrichment Control System by Catalyst Temperature Estimation to Enable Frequent Stoichiometric Operation at High Engine Speed/Load Condition," in *SAE Technical Paper*, 2013.
[26] A. Cairns, P. Stansfield, N. Fraser, H. Blaxill, M. Gold, J. Rogerson, and C. Goodfellow, "A Study of Gasoline-Alcohol Blended Fuels in an Advanced Turbocharged DISI Engine," *SAE Int. J. Fuels Lubr.*, vol. 2, no. 1, pp. 41–57, Apr. 2009.
[27] *Advanced Direct Injection Combustion Engine Technologies and Development, Volume 2: Diesel Engines (Woodhead Publishing in Mechanical Engineering): H Zhao*. .
[28] D. A. Rothamer and J. H. Jennings, "Study of the knocking propensity of 2,5-dimethylfuran–gasoline and ethanol–gasoline blends," *Fuel*, vol. 98, pp. 203–212, 2012.
[29] L. J. Hamilton, M. G. Rostedt, P. A. Caton, and J. S. Cowart, "Pre-Ignition Characteristics of Ethanol and E85 in a Spark Ignition Engine," *SAE Int. J. Fuels Lubr.*, vol. 1, pp. 145–154, 2008.
[30] S. C. Johnston, C. W. Robinson, W. S. Rorke, J. R. Smith, and P. O. Witze, "Application of Laser Diagnostics to an Injected Engine," in *SAE Technical Paper*, 1979.
[31] G. M. Rassweiler and L. Withrow, "Motion Pictures of Engine Flames Correlated with Pressure Cards," Jan. 1938.
[32] C. D. Miller, "Relation between spark-ignition engine knock, detonation waves, and autoignition as shown by high-speed photography," in *NACA Report*, 1946, no. 855.
[33] G. Konig and C. G. W. Sheppard, "End Gas

Autoignition and Knock in a Spark Ignition Engine," in *SAE Technical Paper*, 1990.
[34] J. B. Heywood, *Internal Combustion Engine Fundamentals*. 1988.
[35] H. R. Ricardo, "Paraffin as Fuel," *Automob. Eng.*, 1919.
[36] W. Fickett and W. C. Davis, *Detonation: theory and experiment*. Courier Corporation, 2012.
[37] R. Maly, R. Klein, N. Peters, and G. Kðnig, "Theoretical and Experimental Investigation of Knock Induced Surface Destruction," *SAE Tech. Pap.*, p. 41, 1990.
[38] G. G. Zhu, I. Haskara, and J. Winkelman, "Stochastic Limit Control and Its Application to Knock Limit Control Using Ionization Feedback," in *SAE Technical Paper*, 2005.
[39] N. S. Lightfoot and C. R. Negus, "Investigation of the 'knock' phenomenon in an optically-accessed engine," *Symp. Combust.*, vol. 20, no. 1, pp. 111–122, Jan. 1985.
[40] F. Yang, H. Zhang, Z. Chen, and W. Kong, "Interaction of pressure wave and propagating flame during knock," *Int. J. Hydrogen Energy*, vol. 38, no. 35, pp. 15510–15519, Nov. 2013.
[41] N. Kawahara and E. Tomita, "Visualization of auto-ignition and pressure wave during knocking in a hydrogen spark-ignition engine," *Int. J. Hydrogen Energy*, vol. 34, no. 7, pp. 3156–3163, 2009.
[42] K. G., *Autoignition and Knock Aerodynamics in Engine Combustion.* Leeds, UK : Department of Mechanical Engineering, The University of Leeds, 1993.

فصلنامهٔ علمی- پژوهشی تحقیقات موتور

تارنمای فصلنامه: www.engineresearch.ir

تصویر برداری و تحلیل خود اشتعالی و کوبش در موتور شیشه‌ای

حسن وفامهر[۱و۲*]، امین محمودزاده اندواری[۲]، وحید اصفهانیان[۳]، قدرت‌الله حمزه نوا[۴]

[۱] پژوهشگر دانشکده مهندسی مکانیک دانشگاه ناتینگهام، انگلستان، h.vafamehr@ut.ac.ir

[۲] پژوهشگر دانشکده مهندسی مکانیک دانشگاه تهران، تهران، ایران، amin.mahmoudzadeh@ut.ac.ir

[۳] عضو هیات علمی دانشکده مهندسی مکانیک دانشگاه تهران، تهران، ایران evahid@ut.ac.ir

[۴] دانشکده مهندسی مکانیک، دانشگاه تهران، تهران، ایران hamzehnava@ut.ac.ir

* نویسندهٔ مسئول

چکیده

این مقاله به موضوع مطالعه درباره پیش جرقه در شرایط کوبش موتور پرداخته موتور مورد استفاده در این تحقیق از نوع تک استوانه با قابلیت دسترسی کامل تصویری از بالای استوانه است. این موتور می تواند حداکثر فشار ۱۵۰ بار را در شرایط سخت تحمل کند. شرایط کوبش در فشار پایین ۵ بار و با استفاده از گرم کن هوای ورودی و استفاده از سوخت با عدد اکتان ۷۵ به موتور تحمیل شد. در این مقاله دوربین عکاسی تندنگار (۶۰،۰۰۰ عکس در ثانیه) به همراه آنالیز اطلاعات حرارتی دریافتی از موتور کمک به تحلیل اتفاقات احتراق می کند مهمترین دستاورد این تحقیق ، بهبود درک از احتراق خودکار و مرکزهای متعدد آن در شرایط کوبش سخت می باشد. دیده شدن مرکزهای پراکنده جرقه دو محفظهٔ احتراق همسو با نظریه توسعه انفجار است. بررسی ترمودینامیکی اطلاعات نشان دهنده این است که بین شدت کوبش و مقدار سوخت مشتعل نشده در لحظه شروع کوبش ارتباطی وجود ندارد. همچنین بررسی عکس های گرفته شده در چرخه های بعد از کوبش شدید موتور، قطرات ریز روغن در محفظهٔ احتراق دیده می شود که همین باعث شروع پیش از موقع احتراقی باشد. این پدیده تاثیر مستقیم با رفتار نوسانی کوبش دارد. در نهایت نتایج بدست آمده نشان دهنده رابطهٔ مستقیم بین دمای مناطق مختلف موتور و خود اشتعالی است.

اطلاعات مقاله

تاریخچهٔ مقاله:

دریافت: ۱۴ دی ۱۳۹۸

پذیرش: ۲۹ بهمن ۱۳۹۸

کلیدواژه‌ها:

کوبش

خود اشتعالی

تصویر برداری